# Theoretical analysis of the magnetization and of the paramagnetic and diamagnetic magneto-optical effects in Pr-substituted yttrium iron garnets using quantum theory

Jiehui Yang
*Department of Physics, Nanjing University, Nanjing 210008, China*
*and Luoyang Teacher's College, Luoyang 471022, China*

You Xu
*China Center for Advanced Science and Technology (World Laboratory), P.O. Box 8730, Beijing 100080, China;*
*Department of Physics, Nanjing University, Nanjing 210008, China;*
*and State Key Laboratory of Magnetism, Institute of Physics, Chinese Academy of Sciences, Beijing 100080, China*

Fang Zhang
*Department of Physics, Nanjing University, Nanjing 210008, China*
*and Luoyang Teacher's College, Luoyang 471022, China*

Maurice Guillot
*Laboratorie des Champs Magnétiques Intenses, CNRS/MPI, 38042 Grenoble, France*
(Received 18 March 1997)

By using quantum theory, the magneto-optical (Faraday rotation, Faraday ellipticity) properties at photon energies below 6 eV and the magnetic properties of the $Pr^{3+}$ ion in the $Y_3Fe_5O_{12}$ garnet are analyzed in the 50–300 K temperature range. The strong enhancement of the Faraday rotation induced by the Pr presence originates mainly from the intraionic electrical dipole transitions between the split $4f^2$ and $4f5d$ levels. It is shown that the most important factor is the Pr-Fe superexchange interaction: if there is no Zeeman effect, no magneto-optical (MO) effects exist. The ''paramagnetic'' and ''diamagnetic'' contributions to the MO properties are discussed in detail: if only the Zeeman effect on the ground state is taken into account, the paramagnetic term which is strongly temperature dependent is obtained; on the contrary, if only the Zeeman effect on the excited configuration is considered, the diamagnetic contribution which is temperature insensitive is present. The observed MO properties result from these two components but are mainly determined by the paramagnetic one; the MO resonance frequencies are related to the energies of the multiplets of the ground term and of the excited configuration and to the crystal-field splitting of all these multiplets. Using this approach, the theoretically calculated results of both Pr magnetization and MO effects are in good agreement with experimental data. It is shown that the simultaneous treatment of the magnetic and MO phenomena is a powerful tool to prove the correctness of the approach and of the so-determined parameters. Finally, it is demonstrated that the mixing of the different multiplets of the ground term has a great influence on both magnetic and MO properties. [S0163-1829(97)08038-7]

## I. INTRODUCTION

Magneto-optical (MO) effects have been observed in different types of materials including metals, semimetals, semiconductors and also ferrimagnets, antiferromagnets, ferromagnets, and a large variety of paramagnetic ions imbedded in solids. In metals, semimetals, and semiconductors, MO properties reveal intraband (free carriers) and interband absorption and dispersion. In ionic magnetic solids, the atomic character of the valence electron disappears into energy bands while the remaining unfilled inner shells are strongly affected by spin-orbit coupling, electric crystalline field effects, magnetic exchange (or superexchange) interactions, and important polarized transitions between the final energy levels can arise. Experimental studies are usually performed in transmission and reflection in one of two configurations: Faraday configuration with the wave vector **q** parallel to the external magnetic field **H** (or to the magnetization **M**) and the Voigt (Cotton-Mouton) configuration ($\mathbf{q}\perp\mathbf{H}$ or $\mathbf{q}\perp\mathbf{M}$). It should be noted that although in paramagnetic and diamagnetic materials, MO effects are observed under application of $H$ only, in magnetically ordered crystals MO properties are associated with the inherent spin structure, and can be observed in the absence of **H**.

The spin-photon or MO interactions may be separated either into scattering and absorption processes or into magnetic and electric dipole transitions, or into interactions via one or two magnetic ions; these three groups may be then divided into first- and second-order MO effects. For example, in the microwave range, the para- and ferromagnetic resonances are related to a one magnetic ion-photon interaction whereas in the ferri, antiferro, and exchange resonances, a spin-photon interaction via two magnetic ions is involved. In the visible range, the circular magnetic birefringence (Faraday effect) is a first-order interaction and the linear magnetic birefringence (Cotton-Mouton or Voigt effect) is a second-order coupling. The first classification is well illustrated by the well-known Kramers-Kronings relations which connect scattering and ab-

 

sorption processes like the Faraday (Voigt) effect with circular (linear) magnetic dichroism.[1–3]

In a schematic description of the Faraday (Kerr) rotation, two types of MO phenomena have to be distinguished: ''diamagnetic''-type rotation results from transitions from a nondegenerate ground level to a double-degenerate excited level which is split by some perturbation; ''paramagnetic'' rotation originates from transitions from a double-degenerate ground level which is split by some interaction to a nondegenerate or double-degenerate excited level.

In simple systems, like transition metals Fe, Co, and Ni, it has been shown by Oppeneer *et al.*[4] that the magneto-optical Kerr effect scales linearly with the spin-orbit coupling but is a rather complex function of magnetization (exchange splitting). A similar conclusion about the effect of spin-orbit coupling in the Kerr rotation in MnBi has been deduced by Misemer.[5]

As previously noted, many factors can split the ground and excited states and there exist several kinds of transitions, so the quantum theory has to be used to study the diamagnetic and paramagnetic MO effects. To our knowledge, there is still a lack of the theoretical description of these effects based on the quantum theory and the questions like what kind of transitions, what interaction play the main roles in originating the MO effects, and what is the relative weight of the diamagnetic and paramagnetic MO effects have to be solved. In order to discuss these problems, the MO properties of Pr-substituted iron garnets (Pr:YIG) will be considered, the main reasons for this choice are detailed in the following paragraph.

Within the general formula $\{R_xY_{3-x}\}[Fe_2](Fe_3)O_{12}$ ($R$:YIG), the magnetic and MO properties of the rare-earth (Re)-substituted yttrium iron garnets result directly from the atomic positions of the cubic space group $Ia3d$:$R^{3+}$ and $Y^{3+}$ ions distributed over the dodecahedrally coordinated $\{24c\}$ sites; octahedral sites $[16a]$, and tetrahedral $(24d)$ sites are occupied by the $Fe^{3+}$ ions. The corresponding sublattice magnetizations $M_a$ and $M_d$ are strongly coupled antiferromagnetically because of the strong negative superexchange interactions through the oxygen ions between $Fe^{3+}$ ions on the two sites.[6] As these interactions are not influenced by the $R^{3+}$ ion presence, the Néel temperature is the same (560 K) in all $R$IG's; consequently, the $M_a$ and $M_d$ values are equal to those measured in $\{Y_3\}[Fe_2](Fe_3)O_{12}$ (YIG).[7] In light rare-earth-substituted YIG, the rare-earth sublattice magnetization $M_c$ is, according to the ferrimagnetic arrangement of Néel's model, parallel to the resultant $Fe^{3+}$ magnetization $(M_d-M_a)$, which is usually written as $M_{\mathrm{YIG}}$. So the macroscopic garnet magnetization is simply equal to $M_c+M_{\mathrm{YIG}}$. It should be mentioned that the $R$-Fe superexchange interactions take place mainly between ions of the $\{c\}$ and $[d]$ sites and are of the order of 25 K.[8]

The behavior of the magnetic ions depends not only on the superexchange interactions but also on the crystal field (CF) effect. Because the orbital angular momentum may be fully or partly quenched by CF in the crystal, the ionic magnetic moment is usually, mainly at low temperature, smaller than the free-ion value and may present a strong magnetocrystalline anisotropy.[9] The anisotropies of the superexchange interaction and CF may lead to spin reorientation and (or) to the onset of noncollinear structure in the $\{c\}$ sublattice as observed in some heavy (TbIG, DyIG, ErIG ...) and light (SmIG) iron garnets.[10]

In the garnet series, many ionic substitutions have been studied. But as the garnet structure could not form with a lattice parameter greater than 12.540 Å, the Pr content is limited to 1.33 (value of $x$) in bulk materials.[11,12] However, by using lattice phase epitaxy on high lattice parameter substrates, the maximum amount that Pr in thin films can attain is 1.8.[13] In the visible and infrared bands, the Faraday rotation (FR) of Pr:YIG was observed as strongly negative whatever $x$ is, contrary to the Faraday rotation of YIG, which is considered as positive.[14] To separate the light rare-earth contribution to the Faraday rotation, the hypothesis where the contribution of the two $Fe^{3+}$ sublattices is the same in all $R$IG's was used, since in these bands, the $Fe^{3+}$ absorption spectrum is only very weakly affected by the substitution of $Y^{3+}$ by $Pr^{3+}$ ions.[15] Furthermore, the magnetic moment $m$ (reported to one $Pr^{3+}$ ion) deduced from Néel's model was found to be nearly independent of the substitution rate. Finally, it was concluded that the single-ion model was a good approximate description of both the observed magnetic and MO properties.[14,16]

The Pr substitution for yttrium in YIG results in a very strong enhancement of the Faraday rotation which takes place without noticeable changes of the optical absorption.[17,18] Furthermore, it is one of the largest among the trivalent rare-earth ions. It should be noted that a strong increase of the Faraday rotation was also observed in cerium-substituted YIG but because of the limitation of the Ce content (only a few percent) and (or) the possible presence of tetravalent Ce ions, the analysis of both magnetic and MO properties of Ce:YIG is a very delicate challenge. According to a previous work, where theoretical calculation of the $Pr^{3+}$ contribution to the Faraday rotation was based on the quantum theory, the intraionic electric-dipole transitions between the different perturbation split levels of the $4f^2$ and $4f5d$ configurations are of first importance.[19] However, in this previously published paper only the $Pr^{3+}$ contribution to the paramagnetic-type Faraday rotation at 1150 and 633 nm wavelengths was calculated at room temperature. In this work, the following properties of Pr:YIG will be calculated simultaneously: the magnetization, the paramagnetic, and diamagnetic type and the full Faraday rotation and Faraday ellipticity induced by the Pr sublattice. On the one hand, the magnetic behavior originates from the split levels of the ground configuration, on the other hand the MO phenomena depend not only on the splitting of the ground configuration but also on the splitting of the excited configuration, so the comparison with the different experimental data is helpful for studying the origin of the MO effect and magnetization and for determining the correctness of the model and parameters used.

The arrangement of this paper is as follows: in Sec. II the temperature dependence of the Pr magnetic moment is calculated and compared to the experimental data with attention paid to the determination of the crystal-field and exchange parameters. In Sec. III, the origins of the paramagnetic and diamagnetic contributions to the MO effects are analyzed in details; the relative weight of these contributions to the full Faraday rotation is then discussed. The influence of the mixing of the different multiplets of the ground term induced by

CF on both magnetic and MO properties is treated in Sec. IV. In each of these sections, we present first a general theoretical description adapted to the case of the rare-earth ions in insulators and then compare the theoretical and experimental results. Finally, the conclusions issued from this work are given in Sec. V.

## II. CALCULATION OF THE MAGNETIC MOMENT

The magnetic moment of the considered ion is determined by the successive splittings of the ground configuration induced by spin-orbit (SO), crystal-field, superexchange, and external magnetic-field interactions. Usually, the energy gaps between the ground term and the higher-lying terms of the ground configuration are large enough, and the influence of the higher-lying terms to the splitting of the ground term is negligible especially for the lower-lying multiplets. So, only the ground term needs to be considered in the calculation. The strengths of the SO and CF interactions are usually comparable and much larger than those of the superexchange interaction and external magnetic-field perturbations. Finally, the perturbation calculation has to be carried out with the following order of priorities: $\mathcal{H}_{\mathrm{SO}}+\mathcal{H}_{\mathrm{CF}}$ and $\mathcal{H}_{\mathrm{exch}}+\mathcal{H}_{\mathrm{ext}}$; here $\mathcal{H}_{\mathrm{so}}$, $\mathcal{H}_{\mathrm{CF}}$, $\mathcal{H}_{\mathrm{exch}}$, and $\mathcal{H}_{\mathrm{ext}}$ are the spin-orbit coupling, crystal-field, superexchange interaction, and external magnetic-field Hamiltonian, respectively.

At first, the splitting of the ground term induced by the spin-orbit and crystal-field interactions is calculated by solving the following secular equation:

$$\|\langle i|\mathcal{H}_{\mathrm{SO}}+\mathcal{H}_{\mathrm{CF}}|j\rangle-E\,\delta_{ij}\|=0, \tag{1}$$

where the bra and ket include all the states of the ground term multiplets.

If the CF and SO split levels are degenerate, they will be split further by the superexchange interaction or (and) external magnetic field. Then the occupation probability of the various sublevels of each CF and SO split level will differ and this CF and SO split level will have a net contribution to the magnetic moment. For non-Kramers' ions, some (or all) CF and SO split levels may be nondegenerate and such levels do not contribute to the magnetic moment. But if the energy gap(s) between two (or more) CF and SO split nondegenerate levels is (are) small, these levels will be mixed by the superexchange interaction and (or) external fields and the so-mixed levels will now have a non-negligible contribution to the magnetic moment.

For both cases, the correction of $\mathcal{H}_{\mathrm{exch}}$ and $\mathcal{H}_{\mathrm{ext}}$ to high-order perturbation can be obtained by solving the following secular equation:

$$\|\langle i|\mathcal{H}_{\mathrm{SO}}+\mathcal{H}_{\mathrm{CF}}+\mathcal{H}_{\mathrm{exch}}+\mathcal{H}_{\mathrm{ext}}|j\rangle-E\,\delta_{ij}\|=0, \tag{2}$$

where $|i\rangle$ and $\langle i|\mathcal{H}_{\mathrm{SO}}+\mathcal{H}_{\mathrm{CF}}|i\rangle$ are the eigenwave functions and eigenenergies obtained by solving Eq. (1). Because the occupation probabilities of high-lying CF and SO split levels are small, usually only some low-lying levels need be included in Eq. (2). It should be noted that even if the CF and SO split levels are degenerate, the high-order perturbation correction should be taken into account when the energy gaps between different CF and SO split levels are small.

The ionic magnetic moment, at a temperature $T$, is given by

$$m=-\mu_B\sum_g \langle g|(L_z+2S_z)|g\rangle\rho_g, \tag{3}$$

where $|g\rangle$ is the CF-SO split and superexchange-interaction $\mathcal{H}_{\mathrm{ext}}$-mixed (or split) state whose occupation probability is expressed as

$$\rho_g=\exp(-E_g/kT)\Big/\sum_g \exp(-E_g/kT). \tag{4}$$

Néel theory[20] reduces to the assumptions that the superexchange interaction acting on the rare-earth ions in rare-earth iron garnets can be expressed as

$$\mathcal{H}_{\mathrm{exch}}=2\mu_B H_{\mathrm{exch}} S_z, \tag{5}$$

where $H_{\mathrm{exch}}$ is the exchange field and is proportional to the resultant spontaneous magnetization of the $Fe^{3+}$ sublattices $M_{\mathrm{YIG}}$:

$$H_{\mathrm{exch}}=n_0(1+\gamma T)M_{\mathrm{YIG}}. \tag{6}$$

It is noted that, strictly speaking, $n_0$ is not the classical molecular coefficient since the proportionality between the molecular field and $H_{\mathrm{exch}}$ is included in it. Furthermore Eq. (5) can be used at the same time with the same $n_0$ and $\gamma$ values, for all the multiplets of the ground term. $M_{\mathrm{YIG}}$ is temperature dependent and, in this work, values of the $M_{\mathrm{YIG}}$ deduced from the nuclear magnetic resonance experiments by Gonano, Hunt, and Meyer[7] will be used.

The challenge was to fit simultaneously to the temperature dependences of both the magnetic and MO (Faraday rotation and Faraday ellipticity spectra) properties with attention paid to the resonance frequencies below 6 eV photon energy, since in Ref. 19 only the room temperature Faraday rotation have been considered.

At first, the splitting of the ground term induced by the spin-orbit and crystal-field interactions was calculated by solving Eq. (1). Since the $Pr^{3+}$ ion is of the non-Kramers' type, each CF and SO split level is nondegenerate in the $D_2$ symmetry environment. The ground $(4f^2)$ configuration of the free $Pr^{3+}$ ion contains three spin-triplet terms ($^3H$, $^3F$, $^3P$), the $^3H$ term being the ground term. According to the book by Martin, Zalubus, and Hagan,[21] the average energies of these three terms are 2446, 6176, and 22 580 $\mathrm{cm}^{-1}$, respectively, and the energies of the three multiplets $^3H_4$, $^3H_5$, $^3H_6$ of the $^3H$ term are 0, 2152, and 4389 $\mathrm{cm}^{-1}$, respectively. Note that all these values were determined by optical spectroscopy.

The determination of the CF parameters was rapidly found to be a crucial question. In a first attempt, we discovered that the CF parameters calculated by the point-charge model were, several times, too small to fit the Pr:YIG Faraday rotation observed at 1150 and 633 nm wavelengths and at room temperature.[19] From the study of the spin-reorientation in SmIG, Nekvasil *et al.*[22] concluded the same failure of the point-charge model for the $Sm^{3+}$ ion. In our second attempt, we used, as $Pr^{3+}$ CF parameters, the $Sm^{3+}$ values of Ref. 22 with a corrective factor taking into account the difference between the $Pr^{3+}$ and $Sm^{3+}$ radii. Although a reasonable agreement between theoretical values and Faraday rotation room-temperature data was found as previously mentioned in Ref. 19, only a very poor fit of the magnetiza-

TABLE I. The parameters of the CF upon the $Pr^{3+}$ ions in YIG (in $cm^{-1}$).

| | $A_{20}\langle r^2\rangle$ | $A_{2\pm2}\langle r^2\rangle$ | $A_{40}\langle r^4\rangle$ | $A_{4\pm2}\langle r^4\rangle$ | $A_{4\pm4}\langle r^4\rangle$ |
|---|---|---|---|---|---|
| $4f$ | −917 | 353 | −8 413 | 425 | 1 274 |
| $5d$ | −4403 | 1696 | −155 928 | 8020 | 65 180 |
| | $A_{60}\langle r^6\rangle$ | $A_{6\pm2}\langle r^6\rangle$ | $A_{6\pm4}\langle r^6\rangle$ | $A_{6\pm6}\langle r^6\rangle$ | |
| $4f$ | 3066 | −301 | 1085 | 136 | |

tion temperature dependence and of the resonance frequencies was obtained. But as the strong temperature dependence of Faraday rotation has also to be explained, we were constrained to modify the initial set of the CF parameters.

According to Eqs. (2)–(5), it is worth noting that both magnetic and MO properties are influenced not only by the CF parameter set but also by the superexchange field. It is reminded that the set of Ref. 19 has to be associated with an exchange field of 480 kOe at room temperature. Finally, the best fit of all the considered properties leads to the nonzero CF parameters reported in Table I, to $n_0$ equal to $-5.0\times10^4$ Oe/($\mu_B$/one formula of YIG), and to $\gamma$ is $1.85\times10^{-3}$ $K^{-1}$. These values are used in this section and in all the following sections. It is worth pointing out that the sign and the order of magnitude of each nonzero CF parameters are the same as those of Ref. 19.

The energies of the lowest 12 and the highest level of the CF and SO split levels of the ground term obtained by solving Eq. (1) are listed in Table II. The corresponding wave functions of the lowest three levels and the seventh and tenth levels are listed in Table III. From this table, it can be seen that the lowest two levels can be mixed by the superexchange interaction (or $\mathcal{H}_{\rm ext}$), however the third level cannot be mixed with the lowest two levels by the superexchange interaction or $\mathcal{H}_{\rm ext}$. The fourth, fifth, and sixth levels (for simplicity, the wave functions of these levels are not listed in the table) also cannot be mixed with the lowest two levels. The energies of the lowest two higher levels, which can be mixed with the lowest two levels, are 178.4 and 1683.8 $cm^{-1}$. The energy differences between them and the lowest two levels are larger than 1300 $cm^{-1}$, which is so large that the mixing of the lowest two levels with the higher levels induced by the superexchange interaction or $\mathcal{H}_{\rm ext}$ is negligible. So, in calculating the Zeeman effect of the lowest two levels, only these two states were included in Eq. (2) and the effect of other higher levels were neglected. The third level can also be mixed with some other levels and has a contribution to the magnetic moment. However the energy of the third level is about 680 $cm^{-1}$ higher than the second one, the occupation probability of this level is very small. Therefore it was neglected in the calculation of the magnetization and Faraday effect. Because of the same reason other levels were also neglected in the calculation. The so-obtained energies, were functions, average magnetic moments, and occupation probabilities of the lowest two CF-SO split and superexchange-interaction-mixed levels are listed in Table IV.

The calculated magnetic moment with the measured values obtained by Leycuras *et al.*[14] are listed in Table V. Considering the measurement error (20%), the theoretical values are in good agreement with the measured ones except those at low temperatures. This discrepancy may originate from the onset of nonlinear magnetic structures in the $\{c\}$ sublattice as observed for many heavy rare-earth iron garnets.[10]

Now we would like to present some comments about the previous determination of the CF parameters. Many works have been devoted to the crystal-field effects upon the rare-earth ions in various magnetic compounds. For some rare-earth transition-metal intermetallics, the magnetic properties were well interpreted by the CF parameters calculated with the point-charge model but the CF shielding factors were often determined by fitting the experimental data.[23,24] For *R*IG's and rare-earth trifluorides, the parameters of the CF upon the rare-earth ions were deduced generally from either the optical or(and) magnetic data. The sets of CF parameters proposed by different authors are not usually in good agreement[25,26] and it is found that these parameters appear to be strongly sensitive to the nature of the next-nearest neighbors, even though the electric charges of the neighbors are the same.[27,28] Furthermore, attention has to be paid to the set determined in Ref. 19: the changes of the rare-earth nearest- and next-nearest neighbor distances, when passing from SmIG to Pr:YIG, have not been taken into account. From these facts, we can conclude that the set of CF parameters used in this paper, which is obtained according to the $Sm^{3+}$ set of Ref. 22 with the corrective factor mentioned above, and is made to fit both the experimental magnetic and MO (see next sections) data, is reasonable. One reason that the correct values of Faraday rotation at λ equal to 1150 and 633 nm, and at room temperature, can also be explained by using the old set of the CF parameters[19] is as follows: these wavelengths are far from MO resonance frequencies, so the Faraday rotation is not very sensitive to the accurate location of the resonance frequencies.

Now we will have some discussions about the superexchange interaction. The thermal evolution of the exchange-field coefficient, to the first-order approximation, is expressed as $n_0(1+\gamma T)$. The temperature dependence of the exchange-field coefficient is first attributed to the thermal

TABLE II. The energies (in $cm^{-1}$) of the lowest 12 and the highest CF-SO split levels of the ground term of the $Pr^{3+}$ ion.

| | | | | | | | |
|---|---|---|---|---|---|---|---|
| $4f^2$ | −1140.95, | −1123.70, | −448.32, | −82.36, | 105.38, | 145.54, | 178.40 |
| | 260.19, | 269.71, | 1683.81, | 1702.6, | 2028.2, | ...5657.3 | |

TABLE III. The wave functions of the lowest three and the seventh and tenth CF-SO split levels of the ground term of the $Pr^{3+}$ ion. Here and in Tables IV and VII, the representation $|J,J_z\rangle$ is used, so, for example, $|4,3\rangle$ represents the wave function $|J=4,\ M_J=3\rangle$ $(L=5)$.

| Energy ($cm^{-1}$) | Wave function |
|---|---|
| −1140.95 | $-0.696\ 54\|4,3\rangle+0.042\ 84\|4,1\rangle-0.042\ 84\|4,-1\rangle$<br>$+0.696\ 54\|4,-3\rangle$<br>$+0.010\ 95\|5,5\rangle-0.112\ 39\|5,3\rangle-0.002\ 27\|5,1\rangle$<br>$-0.002\ 27\|5,-1\rangle$<br>$-0.112\ 39\|5,-3\rangle+0.010\ 95\|5,-5\rangle+0.001\ 44\|6,5\rangle$<br>$-0.012\ 76\|6,3\rangle$<br>$-0.008\ 13\|6,1\rangle+0.008\ 13\|6,-1\rangle+0.012\ 76\|6,-3\rangle$<br>$-0.001\ 44\|6,-5\rangle$ |
| −1123.70 | $0.692\ 85\|4,3\rangle+0.072\ 38\|4,1\rangle+0.072\ 38\|4,-1\rangle$<br>$+0.692\ 85\|4,-3\rangle$<br>$-0.007\ 57\|5,5\rangle+0.120\ 33\|5,3\rangle+0.004\ 79\|5,1\rangle$<br>$-0.004\ 79\|5,-1\rangle$<br>$-0.120\ 33\|5,-3\rangle+0.007\ 57\|5,-5\rangle-0.000\ 82\|6,5\rangle$<br>$+0.011\ 75\|6,3\rangle$<br>$-0.004\ 51\|6,1\rangle-0.004\ 51\|6,-1\rangle+0.011\ 75\|6,-3\rangle$<br>$-0.000\ 82\|6,-5\rangle$ |
| −448.32 | $0.066\ 45\|4,4\rangle+0.700\ 32\|4,2\rangle+0.051\ 02\|4,0\rangle$<br>$+0.700\ 32\|4,-2\rangle$<br>$+0.066\ 45\|4,-4\rangle-0.016\ 57\|5,4\rangle+0.054\ 22\|5,2\rangle$<br>$+0\|5,0\rangle$<br>$-0.054\ 22\|5,-2\rangle+0.016\ 57\|5,-4\rangle-0.005\ 77\|6,6\rangle$<br>$-0.007\ 76\|6,4\rangle$<br>$+0.022\ 91\|6,2\rangle-0.002\ 86\|6,0\rangle+0.022\ 91\|6,-2\rangle$<br>$-0.007\ 76\|6,-4\rangle$<br>$-0.005\ 77\|6,-6\rangle$ |
| 178.40 | $-0.049\ 83\|4,3\rangle+0.692\ 99\|4,1\rangle+0.692\ 99\|4,-1\rangle$<br>$-0.049\ 83\|4,-3\rangle$<br>$+0.026\ 86\|5,5\rangle-0.128\ 40\|5,3\rangle+0.007\ 70\|5,1\rangle$<br>$-0.007\ 70\|5,-1\rangle$<br>$+0.128\ 40\|5,-3\rangle-0.026\ 86\|5,-5\rangle+0.000\ 64\|6,5\rangle$<br>$+0.000\ 22\|6,3\rangle$<br>$+0.004\ 11\|6,1\rangle+0.004\ 11\|6,-1\rangle+0.000\ 22\|6,-3\rangle$<br>$+0.000\ 64\|6,-5\rangle$ |
| 1683.80 | $-0.115\ 33\|4,3\rangle-0.126\ 32\|4,1\rangle+0.126\ 32\|4,-1\rangle$<br>$+0.115\ 33\|4,-3\rangle$<br>$+0.073\ 17\|5,5\rangle+0.659\ 31\|5,3\rangle+0.127\ 30\|5,1\rangle$<br>$+0.127\ 30\|5,-1\rangle$<br>$+0.659\ 31\|5,-3\rangle+0.073\ 17\|5,-5\rangle-0.035\ 63\|6,5\rangle$<br>$+0.113\ 25\|6,3\rangle$<br>$-0.020\ 00\|6,1\rangle+0.020\ 00\|6,-1\rangle-0.113\ 25\|6,-3\rangle$<br>$+0.035\ 63\|6,-5\rangle$ |

lattice expansion. When we refer to the variation of the exchange integral $A$ versus $(\delta-2r)$ for many $3d$, $4d$, and $4f$ metals or alloys ($\delta$ is the distance between two nearest atoms and $r$ is the orbital radius of the $3d$, $4d$ or $4f$ electronic shell) proposed in 1936 by Néel,[29] it is easily concluded that when temperature increases, the superexchange interaction may be either weakened or enhanced depending on the characteristics of the considered ion and on the ion-next-nearest-neighbor distance. In other words, $\gamma$ may be negative or positive. Furthermore, it should be noted that the above analysis is based on the mean-field approximation, in which no correlation effects are introduced. Generally, these effects are expected to improve the quality of the theoretical analysis; since they are stronger at low temperatures, they will also contribute to the $\gamma$ coefficient in Eq. (6).

Let us now discuss further the difference between the exchange and the classical molecular ($H_m$) fields. In the molecular field approximation, the Zeeman Hamiltoman is written $\mu_B H_m(2S_z+L_z)$, and the molecular field is expressed as $H_m=n_0'(1+\gamma' T)M_{\mathrm{YIG}}$. From the comparison with Eq. (5), we conclude that for one state, the ratio $H_{\mathrm{exch}}/H_m$ is equal to $\langle(2S_z+L_z)\rangle/\langle 2S_z\rangle$, here $\langle S_z\rangle$ represents the expectation value of the operator $S_z$ in this state. When only the ground multiplet is taken into account, this ratio is a constant and the Hamiltonian Eq. (5) and the Hamiltonian $\mu_B H_m(2S_z+L_z)$ are equivalent. But because of the values of $\langle(2S_z$

TABLE IV. The energies (in $cm^{-1}$), occupation probabilities ($\rho_g$), magnetic moment ($m$, in $\mu_B$/ion), and wave functions of the lowest two CF-SO split and superexchange-interaction-mixed levels of the ground term at 294 K.

| Energy | $\rho_g$ | $m$ | Wave function |
|---|---|---|---|
| −1 154.41 | 0.5539 | 2.029 36 | $-0.197\,50\|4,3\rangle+0.075\,71\|4,1\rangle+0.004\,31\|4,-1\rangle$ $+0.963\,44\|4,-3\rangle+0.004\,94\|5,5\rangle-0.027\,14\|5,3\rangle$ $+0.000\,76\|5,1\rangle-0.004\,54\|5,-1\rangle-0.160\,18\|5,-3\rangle$ $+0.013\,31\|5,-5\rangle+0.000\,75\|6,5\rangle-0.004\,14\|6,3\rangle$ $-0.009\,26\|6,1\rangle+0.004\,28\|6,-1\rangle+0.017\,12\|6,-3\rangle$ $-0.001\,65\|6,-5\rangle$ |
| −1 110.19 | 0.4461 | −2.029 36 | $0.962\,41\|4,3\rangle+0.036\,64\|4,1\rangle+0.084\,00\|4,-1\rangle$ $+0.192\,40\|4,-3\rangle-0.012\,36\|5,5\rangle+0.162\,41\|5,3\rangle$ $+0.005\,25\|5,1\rangle-0.002\,74\|5,-1\rangle-0.038\,13\|5,-3\rangle$ $+0.000\,26\|5,-5\rangle-0.001\,47\|6,5\rangle+0.016\,84\|6,3\rangle$ $+0.000\,74\|6,1\rangle-0.008\,25\|6,-1\rangle+0.002\,74\|6,-3\rangle$ $+0.000\,12\|6,-5\rangle$ |

$+L_z)\rangle/\langle 2S_z\rangle$ are different for different multiplets, when the free-ion model ceases to be valid, the relation between the exchange and molecular fields becomes complex mainly because of the mixing of different multiplets by the crystal field (see Sec. IV). Therefore when this mixing cannot be neglected, the superexchange interaction should be expressed by the Hamiltonian Eq. (5) and the exchange field. However, it is expected that the value range of $\gamma$ is more or less alike that of $\gamma'$, though in many rare-earth garnets, the mixing of the different multiplets of the rare-earth ions is not negligible and the value of $\gamma$ is not the same as $\gamma'$ obtained by using $\mu_B H_m(2S_z+L_z)$ as the Zeeman Hamiltonian and neglecting the influence of the higher-lying multiplets. This conclusion explains why the molecular field coefficient and $\gamma'$ values reported by Krinchik *et al.*[30] for Nd, Sm, Gd, Dy, and Yb iron garnets are strongly influenced by the nature of the rare earth, for example, $\gamma'$ varies from $-0.63\times10^{-4}$ (YbIG) to $1.1\times10^{-3}$ $K^{-1}$ (TbIG). Finally, we can conclude that (i) the $\gamma$ value determined for the PrYIG garnet in this work lies in a very reasonable range of magnitude; (ii) our $n_0$ ($-5.0\times10^4$ Oe/($\mu_B$/one formula of YIG) and $\gamma$ ($1.85\times10^{-3}$ $K^{-1}$) values lead to an exchange field which is weakly temperature dependent (−280 to −300 kOe) in the 100–300 K temperature range. The important role of the $\gamma$ value is illustrated through the following numerical examples: according to our calculation, the above-mentioned $n_0$ and $\gamma$ values correspond to a magnetic moment equal to 0.22 (at 294 K) and $0.64\mu_B$ per $Pr^{3+}$ ion (at 100 K), respectively; changing only the $\gamma$ sign ($\gamma=-1.85\times10^{-3}$ $K^{-1}$) and keeping $n_0$ constant lead to a strong decrease of the rare-earth magnetization, which is now equal to 0.060 (at 295 K) and $0.45\mu_B$ per $Pr^{3+}$ ion (at 100 K), respectively, except at very low temperatures.

Finally, it should be pointed out that spin-orbit interaction splitting of the $^3H$ term is about 4000 $cm^{-1}$ as mentioned above, while the splitting induced by the crystal field and by the superexchange interaction are estimated to be 1000 and 50 $cm^{-1}$, respectively. So the order of priority in the perturbation calculation, which is presented at the beginning of this section, can be applied for the analysis of magnetic and MO properties of the $Pr^{3+}$ ions in the garnet structure. We emphasize that both the spin-orbit and crystal-field interactions should be taken as the first perturbation correction, otherwise the mixing of different multiplets induced by the crystal-field cannot be correctly introduced. It will be proved in Sec. IV that such a mixing influences strongly both the magnetic and MO properties.

## III. THE CALCULATION OF FARADAY EFFECTS

For each nonequivalent magnetic site, the specific Faraday rotation and Faraday ellipticity caused by the electric dipole transitions are given, according to Refs. 31 and 32, by

$$\theta_F=\frac{\pi N(n^2+2)^2e^2}{9cn\hbar}\times\sum_{ng}A_{ng}\frac{\omega^2(\omega_{ng}^2-\omega^2-\Gamma_{ng}^2)}{(\omega_{ng}^2-\omega^2+\Gamma_{ng}^2)+4\omega^2\Gamma_{ng}^2}\rho_g, \tag{7}$$

$$\psi=\frac{\pi N(n^2+2)^2e^2}{9cn\hbar}\sum_{ng}A_{ng}\frac{\omega\Gamma_{ng}(\omega_{ng}^2+\omega^2+\Gamma_{ng}^2)}{(\omega_{ng}^2-\omega^2+\Gamma_{ng}^2)+4\omega^2\Gamma_{ng}^2}\rho_g, \tag{8}$$

where

TABLE V. The calculated and measured magnetic moment of a $Pr^{3+}$ ion (in $\mu_B$/ion) at various temperatures. $m^*$ is the calculated value without taking the mixing of different multiplets of the ground term into account.

| $T$ (K) | 294 | 255 | 200 | 150 | 100 | 50 | 4.2 |
|---|---|---|---|---|---|---|---|
| $m$ (cal) | 0.22 | 0.26 | 0.34 | 0.44 | 0.63 | 1.10 | 1.99 |
| $m$ (meas) | 0.25 | 0.25 | 0.34 | 0.41 | 0.56 | 0.90 | 1.56 |
| $m^*$ | 0.18 | 0.21 | 0.28 | 0.36 | 0.52 | 0.92 | 1.73 |

$$A_{ng}=|\langle n|V_-|g\rangle|^2-|\langle n|V_+|g\rangle|^2. \quad (9)$$

In Eqs. (7) and (8), $N$ is the number of ions on each considered site, $\Gamma_{ng}$ are the half-widths of resonance lines, the definition of $|g\rangle$ has been given in Sec. II, which are the split states of the ground configuration with energy $E_g$, $|n\rangle$ are the split states of the excited configuration with energy $E_n$, and $h\omega_{ng}/(2\pi)=E_n-E_g$, $n$ is the mean refractive index of the crystal. $eV_\pm$ are the electric dipole moment operators for right- and left-handed circularly polarized light:

$$eV_\pm=e\sum_k [x(k)\pm iy(k)]. \quad (10)$$

$\rho_g$ is the occupation probability of each state $|g\rangle$. To calculate the Faraday rotation and Faraday ellipticity, besides those of the ground configuration, the CF-SO split and superexchange-interaction- and (or) $\mathcal{H}_{\text{ext}}$-mixed (or split) energy levels and the corresponding wave functions of the excited configuration must be calculated by solving Eqs. (1) and (2), respectively.

As the spin-orbit interaction of the excited configuration is larger than that of the ground configuration, the energies of the lower multiplets of one term in the excited configuration may be below the energies of the higher multiplets of a neighbor term, although the average energy of this latter term is smaller than that of the former. Furthermore, the crystal-field interaction on the excited configuration is larger than that on the ground configuration. Therefore, the mixing of different terms induced by the crystal field is generally important, and consequently when we solve Eq. (1), all the excited configuration terms having a spin-angular momentum quantum number identical to that of the ground term have to be considered. It should be noted that, contrary to the ground configuration, not only the lower levels but also the higher levels of the excited configuration contribute to the MO effects. Finally, for the excited configuration, the energies and wave functions of the CF-SO split and superexchange-interaction- and (or) $\mathcal{H}_{\text{ext}}$-mixed (or split) states are determined by solving Eq. (2), the bra and ket including all the CF and SO split states.

### A. Paramagnetic-type Faraday effects

The MO effects do not exist in absence of the Zeeman effect on both the ground and excited configurations; the reason is that the sum of the values of $A_{ng}$ corresponding to the electric dipole transitions from all the states of any CF and SO split level of the ground configuration to all the states of any CF and SO split level of the excited configuration is equal to zero. The origin of the so-called paramagnetic type Faraday rotation can be summarized as follows. Suppose (i) for the ground configuration, there exist either two nondegenerate CF-SO split states which will be mixed by the superexchange interaction and (or) the external field or two states of a double degenerate CF-SO split level which will be now split by the superexchange interaction and (or) external field [in the following, the two CF-SO split and superexchange-interaction-and (or) $\mathcal{H}_{\text{ext}}$-mixed (split) states will be expressed by $|g1\rangle$ and $|g2\rangle$, respectively]; (ii) the Zeeman effect of the excited configuration is neglected. Now, the value of $A_{ng}$ corresponding to the electric dipole transitions from $|g1\rangle$ to any CF and SO split level of the excited configuration and the value of $A_{ng}$ corresponding to the electric dipole transition from $|g2\rangle$ to the same level of the excited configuration have the same magnitude and are of opposite sign.

In the following, we define $\theta_F(ng)$ and $\psi(ng)$ as the Faraday rotation and Faraday ellipticity induced by the electric dipole transition from one state $|g\rangle$ to one state $|n\rangle$, respectively, given by

$$\theta_F(ng)=\frac{\pi N(n^2+2)^2e^2}{9cn\hbar}A_{ng}\frac{\omega^2(\omega_{ng}^2-\omega^2-\Gamma_{ng}^2)}{(\omega_{ng}^2-\omega^2+\Gamma_{ng}^2)+4\omega^2\Gamma_{ng}^2}, \quad (11)$$

$$\psi(ng)=\frac{\pi N(n^2+2)^2e^2}{9cn\hbar}A_{ng}\frac{\omega\Gamma_{ng}(\omega_{ng}^2+\omega^2+\Gamma_{ng}^2)}{(\omega_{ng}^2-\omega^2+\Gamma_{ng}^2)+4\omega^2\Gamma_{ng}^2}, \quad (12)$$

assuming that the occupation probability of the state $|g\rangle$ is equal to 1.

Now, we return to the two CF-SO split and superexchange-interaction- and (or) $\mathcal{H}_{\text{ext}}$-mixed (split) states of the ground configuration described above. The electric dipole transitions from $|g1\rangle$ and $|g2\rangle$ states to the same $|n\rangle$ state have almost the same resonance frequency. If the difference between these two resonance frequencies is neglected, we have

$$\theta_F(ng1)=-\theta_F(ng2), \quad (13)$$

$$\psi(ng1)=-\psi(ng2). \quad (14)$$

But it is worth noting that the occupation probabilities of $|g1\rangle$ and $|g2\rangle$ states are different, hence we get

$$\theta_F(ng1)\rho_{g1}+\theta_F(ng2)\rho_{g2}\neq 0, \quad (15)$$

$$\psi(ng1)\rho_{g1}+\psi(ng2)\rho_{g2}\neq 0. \quad (16)$$

We conclude that the electric dipole transitions from these two states to the state $|n\rangle$ result in Faraday rotation and Faraday ellipticity. The magnitude of both the Faraday rotation and Faraday ellipticity induced by such transitions depends sensitively on the difference of the occupation probabilities and then on the temperature and are usually named the ''paramagnetic-type'' Faraday rotation and ellipticity.

For the $Pr^{3+}$ ions, the lowest parity allowed excited configuration $(4f5d)$ has the following five spin-triplet terms: $^3F$, $^3G$, $^3H$, $^3D$, and $^3P$ with two of them ($^3H$ and $^3G$) involved in the allowed electric dipole transitions from $(4f^2)$ $^3H$ term. However, the $^3G$ ($^3D$) lowest multiplet lies below the $^3F(^3H)$ highest multiplet and the mixing of various spin-triplet terms induced by CF cannot be neglected. So, in the calculation of the CF splitting of the $4f5d$ configuration, the bra and ket in Eq. (1) have to include all the spin-triplet multiplets. The diagonal matrix element values, $\langle i|\mathcal{H}_{\text{so}}|i\rangle$, were also taken from the book by Martin.[21] The spin-triplet multiplets are split into 105 nondegenerate states by CF; the energies and the wave functions of these levels were determined by using the CF parameters of Table I. The energies were found in the 23 055–97 120 $\text{cm}^{-1}$ range. But because

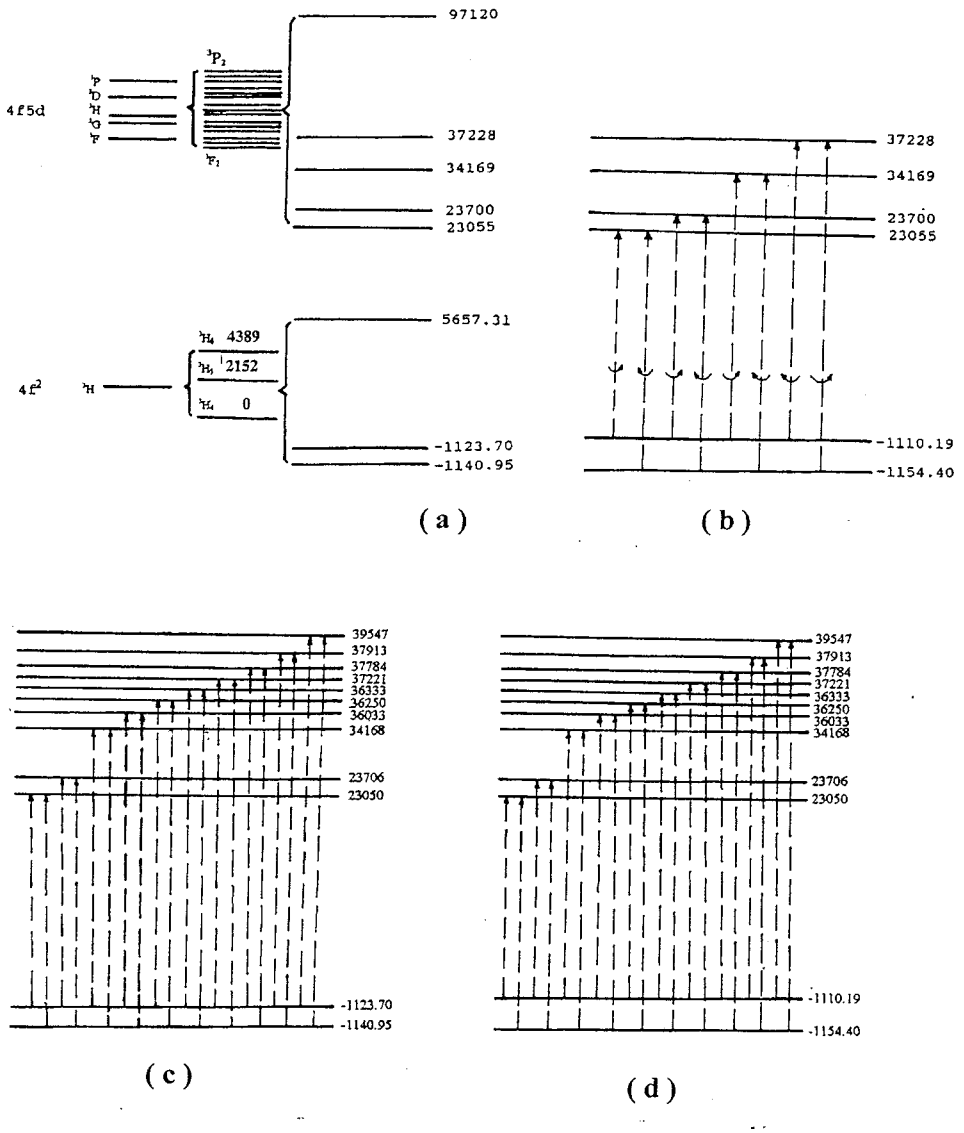


FIG. 1. The split energy levels of the $4f^2$ and $4f5d$ configurations and the electric dipole transitions between them. (a) the energies of some multiplets and CF-SO split levels, no MO transitions between them; (b) the CF-SO split $4f5d$ levels and CF-SO split and superexchange-interaction-mixed $4f^2$ levels, the electric dipole transitions between them result in the paramagnetic Faraday effect; (c) the CF-SO split $4f^2$ levels and CF-SO split and superexchange-interaction-mixed $4f5d$ levels, the electric dipole transitions between them result in the diamagnetic Faraday effects; (d) the CF-SO split and superexchange-interaction-mixed $4f^2$ levels and $4f5d$ levels, the electric dipole transitions between them result in the full Faraday effect.

of the selection rules, only four levels of the excited configuration whose energies are 23 055, 23 700, 34 169, and 37 228 $cm^{-1}$, respectively, yield large contributions to the Faraday rotation and ellipticity below 6.0 eV photon energy (207 nm wavelength). Here the energy of the multiplet $^3H_4$ of the $4f^2$ configuration has been taken as zero. The energies of some multiples and of the CF and SO split levels of both configurations are shown in Fig. 1(a) where, for simplicity's sake, only the levels which will strongly contribute to the MO effects and the highest levels are given. Because the Zeeman effect of both configurations has not been taken into account, the $A_{ng}$ value associated with each electric dipole transition from any nondegenerate CF and SO split $4f^2$ level to any nondegenerate CF and SO split $4f5d$ level is zero and no MO effect exists.

Figure 1(b) shows a summary of our calculations through (i) the most important energy levels of the CF-SO split and superexchange-interaction-mixed $4f^2$ states obtained, at room temperature, by using the exchange-field coefficients determined in Sec. II (we only consider the spontaneous MO effect, so no external magnetic field has been introduced.) (ii) the most important CF and SO split $4f5d$ energy levels; (iii) the electric dipole transitions between them. These transitions result in the paramagnetic Faraday effect. The calculated room-temperature spectra of the Pr contribution to both the specific paramagnetic Faraday rotation and Faraday ellipticity in $Y_2PrFe_5O_{12}$ are shown in Figs. 2 and 3, respectively. Besides the total Faraday rotation and ellipticity, the Faraday rotation and ellipticity produced by the transitions from the lowest two $4f^2$ states to $4f5d$ levels with energies of 23 055, 23 700, 34 169, and 37 228 $cm^{-1}$ are shown as well. Since other $4f5d$ states give small contributions to the MO effects, the total Faraday rotation (ellipticity) is not rigorously equal to the sum of the contributions of the four states. Because the

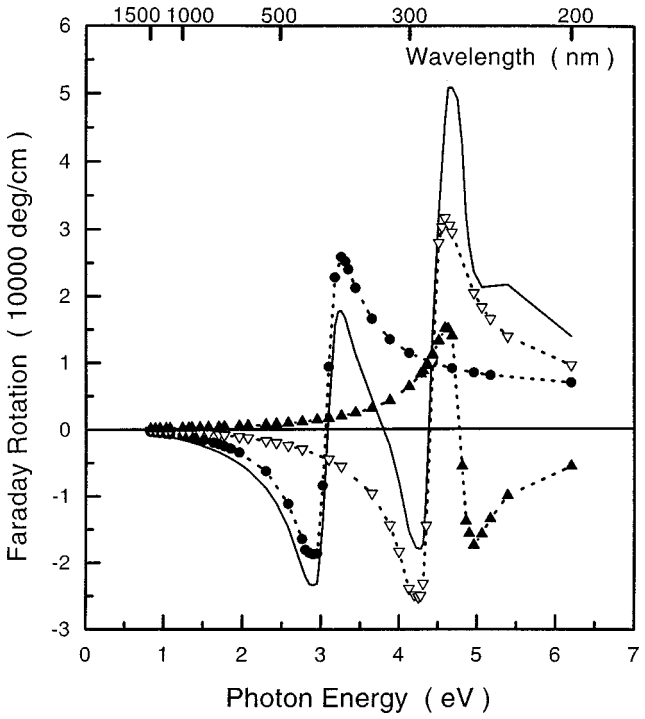


FIG. 2. The paramagnetic-type Faraday rotation spectrum contributed by the $Pr^{3+}$ ions in $Y_2PrFe_5O_{12}$ at 294 K. -●-● Faraday rotation caused by the $4f5d$ levels with energies 23 055 and 23 700 $cm^{-1} \rightarrow 4f^2$ states transitions; ▽-▽-▽ Faraday rotation caused by the $4f5d$ level with energy 34 169 $cm^{-1} \rightarrow 4f^2$ states transitions; -▲-▲-▲ Faraday rotation caused by the $4f5d$ level with energy 37 228 $cm^{-1} \rightarrow 4f^2$ states transitions;—total Faraday rotation.

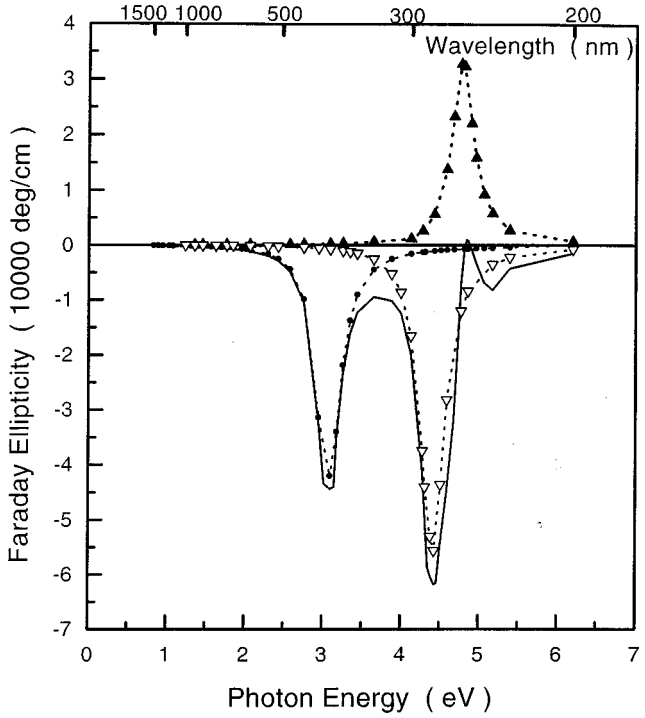


FIG. 3. Same as Fig. 2, but for Faraday ellipticity.

resonance frequencies of the two of these transitions (from the $4f^2$ states to $4f5d$ levels with energies: 23 055 and 23 700 $cm^{-1}$) are nearly the same, only the sum of the contributions of these two transitions is given in the Figs. 2 and 3.

The value of $A_{ng}$ related to the electric dipole transition from the lowest $4f^2$ level (its energy is $-1154.4\ cm^{-1}$) to the $4f5d$ level located at 37 228 $cm^{-1}$ is positive, but the $A_{ng}$ values of the transitions from the same level to other three $4f5d$ levels mentioned above are negative. Therefore, the peaks in the Faraday ellipticity spectrum contributed by the $4f5d$ levels with energies 23 055, 23 700, and 34 169 $cm^{-1}$ are negative, while the peak contributed by the level with energy 37 228 $cm^{-1}$ is positive as shown in Fig. 3 (please note that the first peak in the Faraday ellipticity spectrum is produced by the two $4f5d$ levels with energies 23 055 and 23 700 $cm^{-1}$). The shape of the Faraday rotation spectrum contributed by the $4f5d$ level located at 37 228 $cm^{-1}$ is also different from those induced by other $4f5d$ levels as shown in Fig. 2. According to the values determined by Kucera, Bok, and Nitsch[33] and Gomi, Furuyama, and Abe,[34] in our calculation, the value of $h\Gamma_{ng}/(2\pi)$ is taken to be 0.17 eV for all the MO transitions. The values of $\langle r \rangle_{4f5d}$ and $n$ of YIG, which is only moderately changed by the rare-earth substitution, are taken from Refs. 35 and 36, respectively.

### B. Diamagnetic-type Faraday effects

As we did for the paramagnetic-type Faraday rotation, the so-called diamagnetic-type Faraday rotation originates from the following situation. Suppose (i) The Zeeman effect of the ground configuration is neglected; (ii) in the excited configuration, either two nondegenerate CF and SO split states or two states of a double degenerate CF and SO split level are present. Theses two stats will be mixed with each other or split by the superexchange interaction and (or) external fields. In the following, we use $|n1\rangle$ and $|n2\rangle$ to express these two CF-SO split and superexchange-interaction- and (or) $\mathcal{H}_{\text{ext}}$-mixed (split) states. The $A_{ng}$ values corresponding to the electric dipole transitions from a nondegenerate CF and SO split state $|g\rangle$ of the ground configuration to $|n1\rangle$ and $|n2\rangle$ states have the same magnitude and are of opposite sign. Therefore the absolute value of the Faraday rotation $\theta_F(n1g)\rho_g$ and $\theta_F(n2g)\rho_g$ have the same functional relation with $\omega$, but the resonance frequencies $\omega_{n1g}$ and $\omega_{n2g}$ of these two transitions are slightly different. Then the variation of the sum of $\theta_F(n1g)\rho_g$ and $\theta_F(n2g)\rho_g$ versus the wavelength presents a narrow peak.

To calculate the diamagnetic Faraday rotation in Pr:YIG, we need first to determine the strength of the superexchange interaction on the exited configuration. The average space expansion of the $5d$ wave function is larger than that of the $4f$ wave function, and the superexchange interaction of the $Fe^{3+}$ ions with the $5d$ electron of the $Pr^{3+}$ ions is larger than that with the $4f$ electrons of the $Pr^{3+}$ ions. To our knowledge, there is no theoretical or experimental informations about the magnitude of the interaction involving the $5d$ electrons. In our calculation the superexchange interaction acting on the $5d$ electrons has been estimated to be four times stronger than that on the $4f$ electrons at the same tempera-

ture. The energies and the wave functions of the CF-SO split and superexchange-interaction-mixed states of the $4f5d$ configuration were determined by solving Eq. (2), where all the 105 CF and SO split states were included.

In Fig. 1(c), the lowest two CF-SO split $4f^2$ levels, the most important CF-SO split and superexchange-interaction-mixed $4f5d$ levels, and the different associated electric dipole transitions are schematically shown at room temperature. When only the lowest $4f^2$ state is considered, the $A_{ng}$ values associated with the electric dipole transitions from this state to the CF-SO split and superexchange-interaction-mixed $4f5d$ states with energies 23 050 and 23 706 $cm^{-1}$ were found to be equal to $-2.48\times10^{-2}\times(\langle r\rangle_{4f5d})^2$ and $2.45\times10^{-2}\times(\langle r\rangle_{4f5d})^2$, respectively. Because the two states are not only mixed with each other but also weakly mixed with other states by the superexchange interaction, their absolute values are not rigorously identical. As there exists a very small difference between the resonance frequencies of these two transitions, the sum of the two Faraday rotation contributions leads to a first narrow peak in the Faraday rotation spectrum near 3.0 eV.

Now let us consider the second split $4f^2$ state. As shown in Table III, it is clear that the characteristics of the wave functions of the lowest two CF and SO split $4f^2$ states are very similar. So the $A_{ng}$ values related to the transitions between the second split $4f^2$ state and the split $4f5d$ states having energies of 23 050 and 23 706 $cm^{-1}$ are equal to $-2.49\times10^{-2}\times(\langle r\rangle_{4f5d})^2$ and $2.47\times10^{-2}\times(\langle r\rangle_{4f5d})^2$, respectively. These values are very near those calculated for the lowest split $4f^2$ state. Because the occupation probability of the second $4f^2$ state is slightly different from that of the first state, the transitions issued from the second level also have a contribution to the first peak previously determined at 3.0 eV, but with a smaller magnitude compared with that contributed by the lowest $4f^2$ state as shown in Fig. 4. A second peak at higher photon energy (4.5 eV) originates from various transitions between the lowest two CF and SO split $4f^2$ states and the CF-SO split and superexchange-interaction-mixed $4f5d$ states whose energies are 34 168, 36 032, 36 250, 36 332, 37 221, 37 783, 37 913, 39 546 $cm^{-1}$, respectively [Fig. 1(c)]. Finally in Fig. 4 are reported the contributions, at room temperature, to the diamagnetic-type Faraday rotation spectra of (i) transitions from the lowest CF and SO split $4f^2$ level to the CF-SO split and superexchange-interaction-mixed $4f5d$ levels; (ii) transitions from the second CF and SO split $4f^2$ level to the CF-SO split and superexchange-interaction-mixed $4f5d$ levels. The resultant diamagnetic Faraday rotation spectrum is given as well. The diamagnetic Faraday ellipticity spectra, calculated at the same conditions, are shown in Fig. 5. These figures reveal that the diamagnetic Faraday rotation reaches a maximum value of about $1.8\times10^4$ deg $cm^{-1}$ near 3 and 4.5 eV. However, the peaks are very narrow; therefore, the diamagnetic Faraday rotation is important only in the vicinity of these peaks. It is noticeable that the peaks of the diamagnetic Faraday ellipticity are broader (Fig. 5).

At the end of this section, we would like to emphasize that the values of the diamagnetic type Faraday rotation and Faraday ellipticity have been calculated assuming that the superexchange interaction acting on the $5d$ electrons is four times stronger than that on the $4f$ electrons. However, the order of magnitude of the so-determined values is correct although the precise values of the Faraday rotation and the Faraday ellipticity are sensitive to our choice; for example,

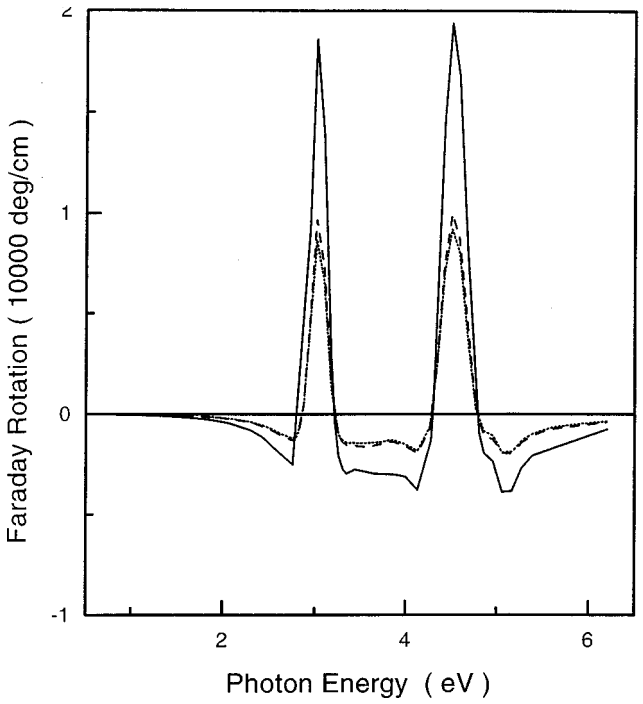


FIG. 4. The diamagnetic-type Faraday rotation spectrum contributed by the $Pr^{3+}$ ions in $Y_2PrFe_5O_{12}$ at 294 K. ----- Faraday rotation caused by the lowest $4f^2$ state$\rightarrow 4f5d$ states transitions; ..... Faraday rotation caused by the second $4f^2$ level$\rightarrow 4f5d$ states transitions; please note the above two curves are very near;—total Faraday rotation.

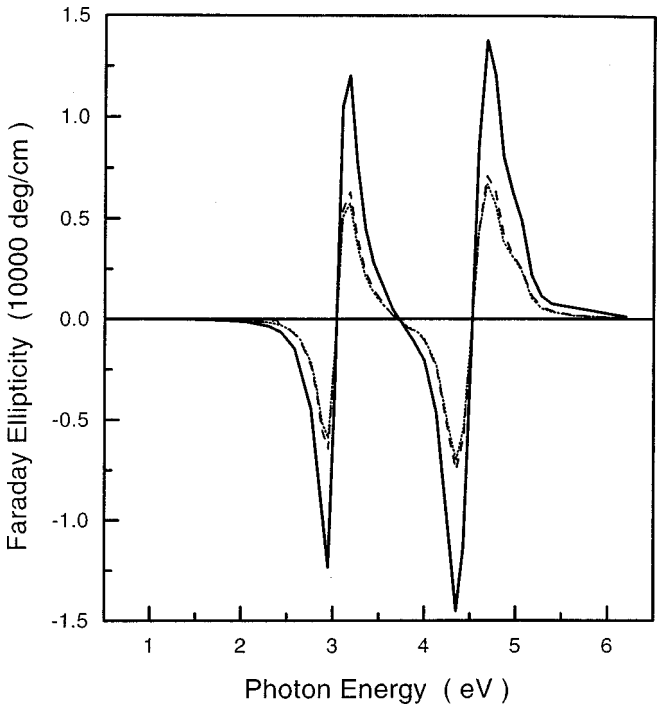


FIG. 5. Same as Fig. 4, but for Faraday ellipticity.

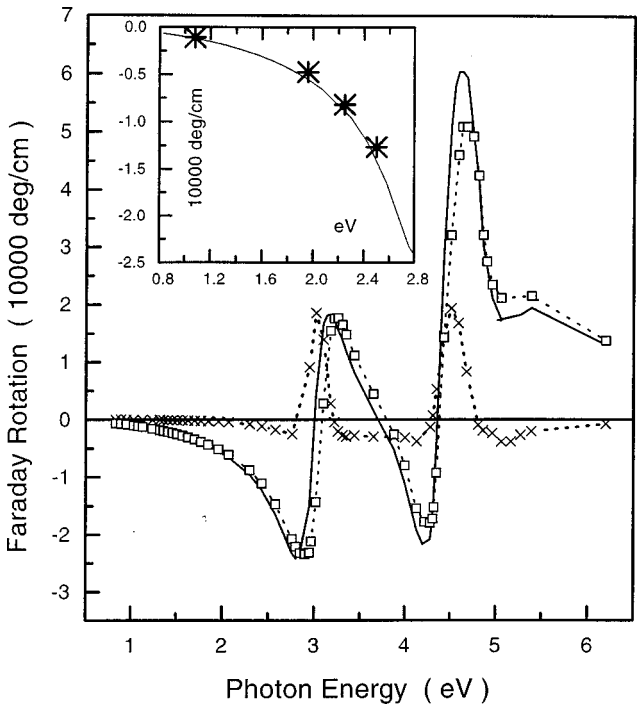


FIG. 6. The Faraday rotation spectrum caused by the $Pr^{3+}$ ions in $Y_2PrFe_5O_{12}$ at 294 K. □-□-□ paramagnetic Faraday rotation caused by the transitions between the CF-SO split and superexchange-interaction-mixed $4f^2$ levels and the CF-SO split $4f5d$ levels; ×-×-× diamagnetic Faraday rotation caused by the transitions between the CF-SO split $4f^2$ levels and the CF-SO split and superexchange-interaction-mixed $4f5d$ levels;—full Faraday rotation caused by the transitions between the CF-SO split and superexchange-interaction-mixed $4f^2$ and $4f5d$ levels. ∗ in the inset represents experimental values.

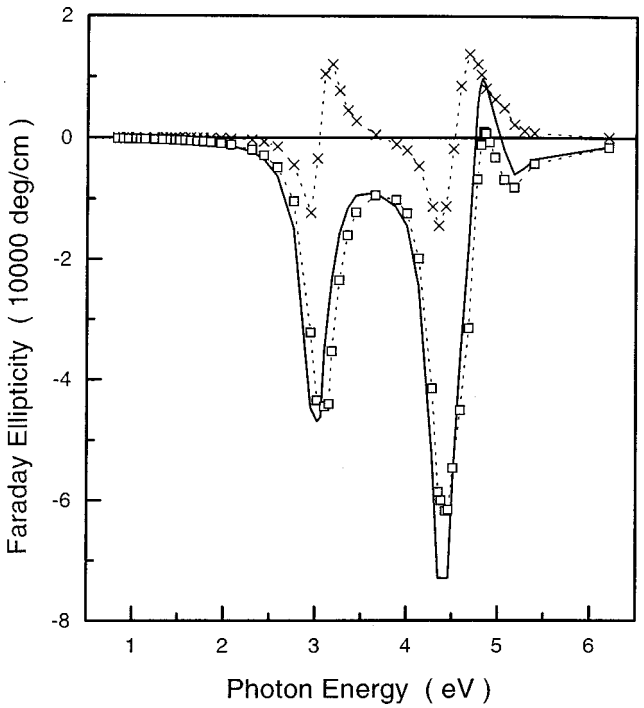


FIG. 7. Same as Fig. 6, but for Faraday ellipticity.

the maximum of the diamagnetic Faraday rotation may vary from about 1 to $2.5\times10^4$ deg $cm^{-1}$ when the ratio of the superexchange interaction changes from 2 to 8. It is also worth noting that the resonance frequencies are only very weakly affected by the choice of this ratio.

### C. Full Faraday effects

When the Zeeman effect of both the ground and excited configurations is taken into account, the full Faraday effects result. Figure 1(d) shows the electric dipole transitions between the CF-SO split and superexchange-interaction-mixed $4f^2$ and $4f5d$ states of the $Pr^{3+}$ ion, which produce the full Faraday rotation. In Fig. 6, the Pr-induced specific paramagnetic, diamagnetic, and full Faraday rotation spectra of $Y_2PrFe_5O_{12}$ at 294 K are plotted, whereas similar contributions to the Faraday ellipticity spectra are given in Fig. 7. The stars in the inset of Fig. 6 represent the experimental values of different authors. From these figures it is concluded that the full Faraday effects are, on the one hand, approximately equal to the sum of the paramagnetic and diamagnetic Faraday effects, and on the other hand, mainly determined by the paramagnetic component. The effect of the diamagnetic Faraday rotation component only induces a very small shift of the peaks in Faraday rotation and Faraday ellipticity spectra.

For non-Kramers' ions, if simultaneously in the ground configuration, the lowest CF and SO split level is nondegenerate and the energy differences between this level and other levels are large enough that the mixing of this level with other levels by the superexchange interaction or external magnetic field is very small, the observed Faraday rotation will be mainly of the diamagnetic type. However, when the material is used in a suitable wavelength range, the Faraday rotation is still important and is nearly temperature independent if we consider that the superexchange interaction temperature variations are negligible.

### D. Comparison with experiments

As noted in the introduction of this paper, the experimental Faraday rotation (FR) data were analyzed in the frame of the one-ion model within the hypothesis of Ref. 14: the resultant $Fe^{3+}$ contribution to the Faraday rotation is given by the values measured in the same experimental conditions on YIG. The $Pr^{3+}$ contribution, which was found proportional to the Pr content, is simply written as

$$\mathrm{FR(Pr)}=\mathrm{FR(Pr{:}YIG)}-\mathrm{FR(YIG)}. \tag{17}$$

At 633 nm wavelength, it was concluded, from the study of epitaxial garnet thin films, that $d\mathrm{FR}/dx$ was equal to $-4700$ and $-15\,800$ deg $cm^{-1}$ at 295 and 4.2 K, respectively,[37] the room-temperature value being confirmed some years later by Gomi, Furuyama, and Abe.[34] At 1150 nm wavelength, the Faraday rotation has been measured on single crystals in the 4.2–300 K temperature range for three Pr contents ($x=1.12\pm0.05$, $0.72\pm0.04$, and $0.32\pm0.05$).[14,16]

At room temperature, the calculated values of specific full Faraday rotation (when $x=1$) is $-5200$ deg $cm^{-1}$ at 633 nm and $-1200$ deg $cm^{-1}$ at 1150 nm, respectively. They are

TABLE VI. Faraday rotation ($\vartheta_F$) calculated and measured values (in $10^3$ deg cm$^{-1}$) at two wavelengths contributed by $Pr^{3+}$ ions in $Y_2PrFe_5O_{12}$ is the calculated value without taking the mixing of different multiplets into account.

| $T$ (K) | $\theta_F$ (cal) 633 nm | $\theta_F$ (cal) 1150 nm | $\theta_F$ (meas) 1150 nm | $\theta_F^*$ 633 nm | $\theta_F^*$ 1150 nm |
|---|---|---|---|---|---|
| 294 | −5.17 | −1.17 | −0.942 | −3.84 | −0.88 |
| 255 | −6.27 | −1.42 | −1.02 | −4.68 | −1.08 |
| 200 | −8.23 | −1.86 | −1.18 | −6.18 | −1.42 |
| 150 | −10.9 | −2.46 | −1.36 | −8.23 | −1.89 |
| 100 | −15.7 | −3.54 | −1.73 | −11.9 | −2.72 |
| 50 | −27.3 | −6.15 | −2.30 | −20.8 | −4.78 |

close to the experimental values obtained by different authors: on the one hand $-4700$ deg cm$^{-1}$ (Ref. 37) $-4800$,[34] on the other hand $-1100$ deg cm$^{-1}$ (Ref. 34) at 633 and 1150 nm, respectively. It is worth noting that Visnovsky *et al.*[38] proposed Faraday rotation values (for $x=1$) of $-8200$ and $-12\,700$ deg cm$^{-1}$ at 2.25 and 2.5 eV, respectively, and as shown in Fig. 6, these estimations are in good agreement with our calculations. According to our calculation, there are three resonance frequencies in the Faraday effect spectra at 3.0, 4.4, and 4.85 eV, respectively (see Fig. 7). Visnovsky *et al.*[38] divided the Faraday rotation into two components: a paramagnetic one and another diamagnetic one and then deduced from the least-squares fit to the diamagnetic component that $\omega_{ng}$ lies in the 3.1–3.3 eV range. At higher energies, to our knowledge, no measurements of Faraday rotation have been performed. However, on the polar Kerr rotation spectrum of Pr:YIG, Visnovsky *et al.*[39] have noted the presence of three peaks at 2.9, 4.3, and 4.85 eV, respectively at room temperature. As the location of the peaks of the Kerr rotation spectrum should be the same as those of the Faraday ellipticity spectrum, it is concluded that our theoretical resonance frequencies are in good agreement with the observed values.

To complete the test of our theoretical approach, the temperature dependence of the Faraday rotation at 633 and 1150 nm wavelengths has been calculated below room temperature. The values are reported in Table VI and compared with the experimental data obtained at 1150 nm wavelength. Down to 100 K, a reasonable agreement between measured and calculated Faraday rotations is obtained although the absolute values of the theoretical Faraday rotation are larger than the measured ones. However, below about 100 K, the calculated Faraday rotation changes more rapidly than the experimental results as temperature decreases. This discrepancy may be attributed to the onset of noncollinear magnetic structure in the $\{c\}$ sublattice.

The calculated Faraday rotation and Faraday ellipticity spectra at 100 K are given in Figs. 8 and 9 to illustrate the strong increase of both specific full and paramagnetic Faraday rotation and the main role of the paramagnetic compo-

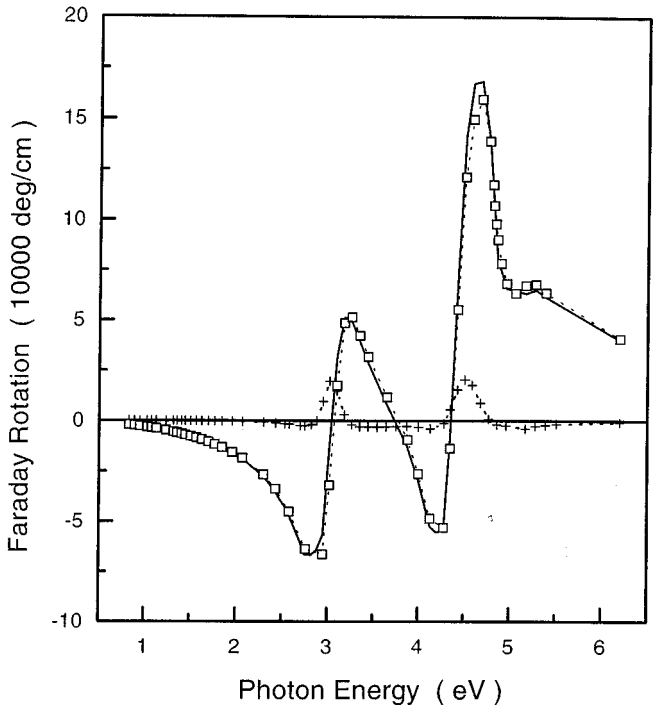


FIG. 8. Same as Fig. 6, but at 100 K.

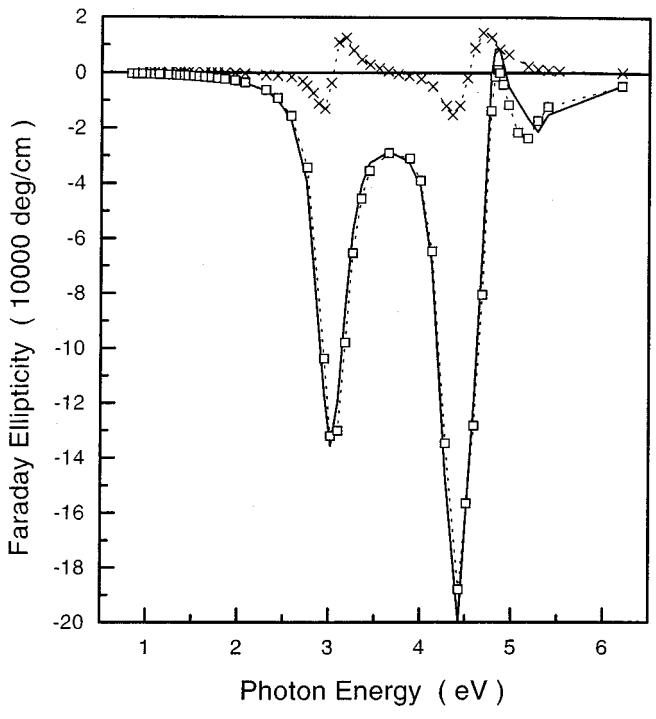


FIG. 9. Same as Fig. 7, but at 100 K.

TABLE VII. The energies (in $cm^{-1}$) and wave functions of the lowest six CF split levels of $(4f^2)\ ^3H_4$ multiplet of the $Pr^{3+}$ ion without taking the mixing of different multiplets into account.

| Energy | Wave function |
|---|---|
| −1067.58 | $-0.704\,18\|4,3\rangle + 0.064\,24\|4,1\rangle - 0.064\,24\|4,-1\rangle + 0.704\,18\|4,-3\rangle$ |
| −1042.00 | $0.699\,82\|4,3\rangle + 0.101\,26\|4,1\rangle + 0.101\,26\|4,-1\rangle + 0.699\,82\|4,-3\rangle$ |
| −427.30 | $0.048\,36\|4,4\rangle + 0.704\,32\|4,2\rangle + 0.056\,37\|4,0\rangle + 0.704\,32\|4,-2\rangle + 0.048\,36\|4,-4\rangle$ |
| 97.07 | $-0.120\,63\|4,4\rangle - 0.696\,74\|4,2\rangle + 0\|4,0\rangle + 0.696\,74\|4,-2\rangle + 0.120\,63\|4,-4\rangle$ |
| 241.21 | $-0.101\,26\|4,3\rangle + 0.699\,82\|4,1\rangle + 0.699\,82\|4,-1\rangle - 0.101\,26\|4,-3\rangle$ |
| 272.63 | $-0.120\,17\|4,4\rangle - 0.031\,14\|4,2\rangle + 0.984\,45\|4,0\rangle - 0.031\,14\|4,-2\rangle - 0.120\,17\|4,-4\rangle$ |

nent. The comparison with data reported in Figs. 6 and 7 confirms that the paramagnetic Faraday rotation is very sensitive to temperature, while the diamagnetic one is not. It should be noted that some of the measured Faraday rotation reported above are the Pr contribution to the Faraday rotation. However some of them correspond to the total Faraday rotation of Pr:YIG because the Fe sublattice contribution, which is much smaller than the rare-earth contribution, can be neglected; furthermore, the Faraday rotation induced by the Fe ions has no MO resonance in the considered wavelength range.

## IV. ROLE OF THE MIXING OF DIFFERENT GROUND TERM MULTIPLETS

Generally in theoretical works on MO effects (see Ref. 40), for the ground configuration, only the lowest-multiplet is considered. However, when higher-lying multiplets of the ground term are taken into account, the energy schema will be modified. Because different multiplets ''repulse each other,'' the energies of all the CF and SO split levels of the lowest multiplet decrease. But these decreases are not uniform, and for the low-lying levels they are smaller than those of higher-lying levels, consequently, the energy gaps between different split levels of the lowest multiplet become smaller. It is remarkable that this situation, which leads to a stronger high-order Zeeman effect, has a great effect on the magnetic and MO properties and, in general, cannot be neglected.

In order to illustrate the role of the ''repulsion'' between different multiplets, the calculation of the magnetization and Faraday effect of the Pr contribution has also been carried out without taking into account such a mixing. In Table VII, the energies and wave functions of the lowest six CF split levels of the $(4f^2)\ ^3H_4$ multiplet determined in the absence of the mixing of this multiplet with $^3H_5$ and $^3H_6$ multiplets are reported. If we remark that the main components of the first nine levels reported in Table II are $^3H_4$ states, we will confirm, by comparing Table VII with Tables II and III, that, because of the ''repulsion'' effect, the energy gap between the lowest two levels becomes smaller when the mixing of different multiplets is considered. Consequently, the mixing of these two CF and SO split levels induced by the superexchange interaction become stronger, hence the difference of the occupation probabilities and the absolute values of the average magnetic moment of these two states increase as shown by the comparison of data in Tables IV and VIII. The absolute values of $A_{ng}$ associated with the electric dipole transitions from these two levels to the split $4f5d$ levels have a similar change as the absolute values of the average magnetic moment. Finally, the introduction of the ''repulsion'' effect, leads to a larger $Pr^{3+}$ contribution to the magnetization and MO effects. By the way, the lowest two levels, obtained with such a mixing, contain very small components of $^3H_5$ and $^3H_6$ multiplets which also influence weakly the magnetization and MO effects. The values of the Pr magnetization calculated without such a mixing, in the

TABLE VIII. The energies (in $cm^{-1}$), occupation probabilities ($\rho_g$), magnetic moment ($m$, in $\mu_B$/ion), and wave functions of the lowest two CF-SO split and superexchange-interaction-mixed levels of the $(4f^2)\ ^3H_4$ multiplet at 294 K without taking the mixing of different multiplets into account.

| Energy | $\rho_g$ | $m$ | Wave function |
|---|---|---|---|
| −1074.97 | 0.5492 | 1.820 55 | $-0.337\,45\|4,3\rangle + 0.101\,36\|4,1\rangle - 0.014\,79\|4,-1\rangle + 0.935\,74\|4,-3\rangle$ |
| −1034.63 | 0.4508 | −1.820 55 | $0.933\,67\|4,3\rangle + 0.064\,08\|4,1\rangle + 0.119\,00\|4,-1\rangle + 0.331\,66\|4,-3\rangle$ |

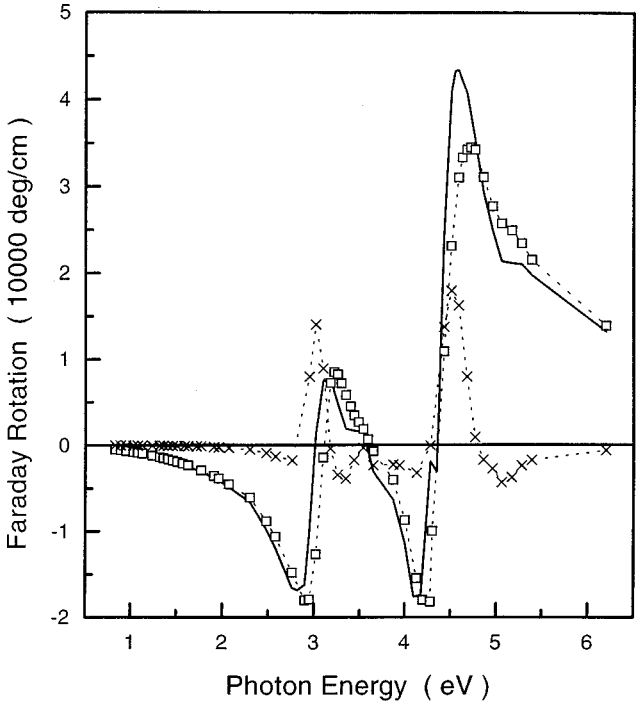


FIG. 10. Same as Fig. 6, but without taking the mixing of the different multiplets of the ground term into account.

4.2–294 K temperature range, are reported in Table V whereas the corresponding values of Pr-induced Faraday rotation at 633 and 1150 nm wavelengths are tabulated in Table VI.

To complete our analysis, we show in Figs. 10 and 11 the calculated Pr-induced diamagnetic, paramagnetic, and full Faraday rotation and Faraday ellipticity at 294 K without taking the repulsion effect into account. By comparing Figs. 10 and 11 with Figs. 6 and 7, it can be seen that such mixing does have a great influence not only on the magnetization (Table V) but also on the MO effects.

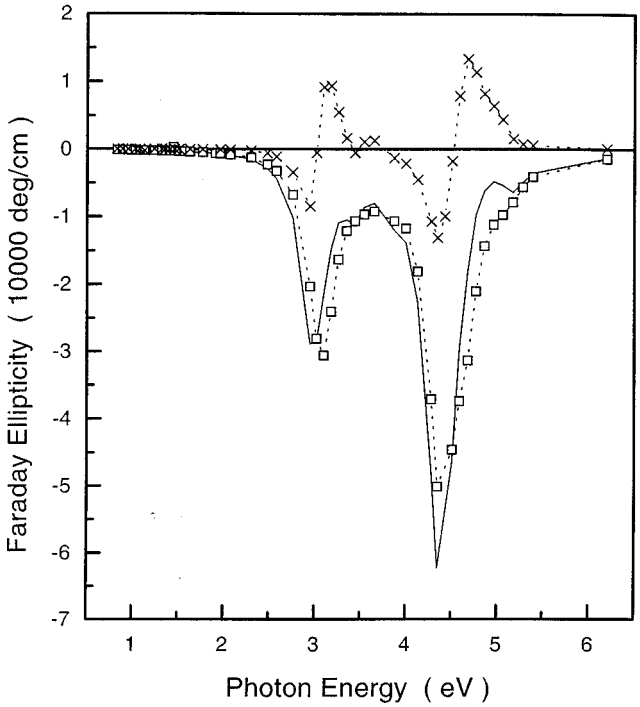


FIG. 11. Same as Fig. 7, but without taking the mixing of the different multiplets of the ground term into account.

## V. CONCLUSION

From the above calculation, the following main conclusions are derived. (1) The Faraday effect contributed by the Pr sublattice in Pr:YIG originates mainly from the intraionic electric dipole transitions between the $4f^2$ and $4f5d$ configurations of the $Pr^{3+}$ ions. (2) The most important factor in the occurring of the Faraday effects is the superexchange interaction or external magnetic field. If there is no Zeeman effect, there will be no Faraday effects. (3) If only the Zeeman effect of the ground configuration is taken into account, while the Zeeman effect of the excited configuration is neglected, the so-called paramagnetic-type Faraday effect will be obtained which depends sensibly on temperature. (4) If we consider the Zeeman effect of the excited configuration but neglect that of the ground configuration, we will obtain the so-called diamagnetic-type Faraday effect which is temperature insensitive. (5) In general, the observed full Faraday rotation contains both components of paramagnetic and diamagnetic Faraday rotations, but it is mainly determined by the paramagnetic Faraday rotation. (6) If the magnetic ions in a material are non-Kramers' ions and if the lowest CF and SO split level of the ground configuration is nondegenerate and is so far from other higher-lying levels that the mixing of this level with other levels induced by the superexchange interaction and external magnetic field is negligible, the observed Faraday effect will be of the diamagnetic type and may be large at suitable wavelengths. In this case, the Faraday rotation will be temperature independent if the superexchange interaction is considered as temperature independent. (7) The MO resonance frequencies are determined by the energy values of the various multiplets of the ground term and of the lowest parity-allowed excited configuration and by the CF splitting of these multiplets. So, besides the ionic characteristics and exchange interactions (external magnetic field), the crystal field is the other important factor which determines the MO behavior of materials. The resonance frequencies are only very weakly affected by the Zeeman effect. (8) The magnetization depends on the splitting of the ground configuration induced by the spin-orbit, crystal field, exchange interactions, and external magnetic field. The temperature dependences of both the magnetization and Faraday effect depend sensibly on the splitting of the ground configuration. (9) For the ground term, the mixing of different multiplets induced by the crystal field has a great influence on both the magnetic and MO properties and cannot be neglected. Furthermore, when the mixings of different multiplets have to be considered for both ground and excited configurations, the exchange field rather than the molecular field should be used to take into account exchange couplings between magnetic ions. The exchange field parameters are not identical to the classical molecular fields coefficients. It is found that the $\gamma$ coefficient for the Pr ion in YIG has to be positive, otherwise the temperature dependences of both

magnetization and Faraday effects would be too strong comparing with the experimental variations. Finally, this work underlines the interest of deducing the crystal-field and exchange parameters simultaneously from the analysis of both magnetic and MO properties.

**ACKNOWLEDGMENTS**

This work has been partly supported by the National Natural Sciences Foundation of China (NSFC) and realized in the frame of an official collaboration between the NSFC and the CNRS of France.

[1] Y. R. Shen, *The Principles of Nonlinear Optics* (Wiley, New York, 1984), p. 13.
[2] F. J. Kahn, P. S. Pershan, and J. P. Remeika, Phys. Rev. **186**, 891 (1969).
[3] H. Le Gall and P. Jamet, Phys. Status Solidi B **46**, 467 (1971).
[4] P. M. Oppeneer, J. Sticht, T. Maurer, and J. Kübler, Z. Phys. B **88**, 309 (1992).
[5] D. K. Misemer, J. Magn. Magn. Mater. **72**, 267 (1988).
[6] J. F. Dillon, *Physics of the Magnetic Garnets*, edited by A. Paoletti (North-Holland, Amsterdam, 1978).
[7] R. L. Gonano, E. Hunt, and H. Meyer, Phys. Rev. **156**, 521 (1967).
[8] M. E. Casperi, A. Koicki, S. Koicki, and G. T. Wood, Phys. Lett. **11**, 195 (1964).
[9] J. Kanamori, in *Magnetism, Vol. 1*, edited by George T. Rado and Harry Suhl (Academic, New York, 1963).
[10] G. F. Dionne, J. Appl. Phys. **47**, 4220 (1976).
[11] G. P. Espinosa, J. Chem. Phys. **37**, 2344 (1962).
[12] S. Geller, Z. Kristallogr. **125**, 1 (1967).
[13] P. Hansen, G. P. Klages, and K. Witter, J. Appl. Phys. **58**, 454 (1985).
[14] C. Leycuras, H. Le Gall, J. M. Desvignes, M. Guillot, and A. Marchand, J. Appl. Phys. **53**, 8181 (1982).
[15] M. Guillot, A. Marchand, H. Le Gall, P. Felmann, and J. M. Desvignes, J. Magn. Magn. Mater. **15–18**, 835 (1980).
[16] C. Leycuras, H. Le Gall, M. Guillot, and A. Marchand, J. Appl. Phys. **55**, 2158 (1984).
[17] G. S. Krinchick and O. B. Esikova, Sov. Phys. Solid State **19**, 2035 (1977).
[18] S. H. Wemple, J. F. Dillon, L. G. Van Uitert, and W. H. Grodkiewiez, Appl. Phys. Lett. **22**, 231 (1972).
[19] Y. Xu, G. Zhang, and M. Duan, J. Appl. Phys. **73**, 6133 (1993).
[20] L. Néel, Ann. Phys. (Paris) **3**, 127 (1948).
[21] W. C. Martin, R. Zalubas, and I. Hagan, *Atomic Energy Levels. The Rare Earth Elements* (National Bureau Standards, Washington, DC, 1978).
[22] V. Nekvasil, M. Guillot, A. Marchand, and F. Tcheou, J. Phys. C **18**, 3551 (1985).
[23] J. E. Greedan and V. U. S. Rao, J. Solid State Chem. **6**, 387 (1973).
[24] Y. Xu, T. Ba, and Y. Liu, J. Appl. Phys. **73**, 6937 (1993).
[25] P. Caro, J. Chem. Phys. **74**, 2698 (1981).
[26] John B. Gruber, Richard P. Leavitt, and Clyde A. Morrison, J. Chem. Phys. **74**, 2705 (1981).
[27] M. Kucera, J. Magn. Magn. Mater. **101**, 242 (1991).
[28] G. Blasse and A. Bril, J. Chem. Phys. **47**, 5139 (1967).
[29] L. Néel, Ann. Phys. (Paris) **5**, 39 (1936).
[30] G. S. Krinchik, V. S. Guskchin, and N. I. Tsidaeva, Sov. Phys. JETP **59**, 410 (1984).
[31] H. A. Kramers, Proc. R. Acad. Sci. Amsterdam **33**, 959 (1930).
[32] Y. R. Shen, Phys. Rev. **133**, A511 (1964).
[33] M. Kucera, J. Bok, and K. Nitsch, Solid State Commun. **69**, 1117 (1989).
[34] M. Gomi, H. Furuyama, and M. Abe, J. Appl. Phys. **70**, 7065 (1991).
[35] S. P. Sinha, *Systematics and the Properties of the Lanthanides* (Springer-Verlag, Berlin, 1983), p. 424.
[36] M. Guillot, P. Feldmann, H. Le Gall, and D. Minella, J. Phys. (Paris) **40**, 883 (1979).
[37] P. Hansen, C. P. Klages, and K. Witter, J. Appl. Phys. **60**, 721 (1986).
[38] S. Visnovsky, V. Prosser, R. Krishnan, V. Parizek, K. Nitsch, and L. Svodokova, IEEE Trans. Magn. **MAG-17**, 3205 (1981).
[39] S. Visnovsky, R. Krishnan, V. Prosser, S. Novak, and I. Bravik, Physica B & C **89**, 73 (1979).
[40] W. A. Crossley, E. W. Cooper, J. L. Page, and R. P. Van Stapele, Phys. Rev. **181**, 896 (1969).